



## A Study on the Macrosatial Correlation Characteristics of Tsunami Wave Height and Tsunami Inundation Depth

Y. Fukutani<sup>(1)</sup>, T. Nakamura<sup>(2)</sup>, T. Shizuma<sup>(3)</sup>

<sup>(1)</sup> Associate Professor, Kanto Gakuin University, [fukutani@kanto-gakuin.ac.jp](mailto:fukutani@kanto-gakuin.ac.jp)

<sup>(2)</sup> Director, Shinozuka Research Institute, Co., Ltd., [naka@shinozukaken.co.jp](mailto:naka@shinozukaken.co.jp)

<sup>(3)</sup> Chief Research Engineer, Shinozuka Research Institute, Co., Ltd., [shizuma@shinozukaken.co.jp](mailto:shizuma@shinozukaken.co.jp)

### Abstract

In a probabilistic disaster risk assessment for multiple buildings, we need to consider hazard correlations among site locations and damage correlations among multiple buildings because the probability distribution of aggregate damage for multiple buildings is affected. Various uncertainties and correlation characteristics, such as ground motion, building response, and material strength, are generally considered in probabilistic seismic risk assessments. However, studies that evaluate the spatial correlation characteristics of tsunamis have yet to be reported. This study aims to elucidate the functional dependency of the spatial correlation coefficients between the tsunami wave heights and tsunami inundation depths on the relative distance between two sites by using linear and nonlinear shallow water equations. First, we established a large virtual fault with a length of 250 km and a width of 100 km in the center of a virtual sea area with a water depth of 1000 m. Using the initial water displacement due to fault movement, we solved the 2D continuous equation and linear long-wave equation with a 500 m grid. The results show that the macrospatial correlation coefficients of the tsunami wave height have a tendency to decrease as the distance increases, but the correlation coefficient was as high as approximately 0.74 even at a distance of approximately 100 km. This trend occurs because there is almost no effect of sea bottom friction or topography that attenuates the tsunami wave height. Second, we constructed the fault parameters of the earthquake in the Sagami trough, which has a large slip off the Kanto area in Japan, to evaluate the spatial correlation coefficients of the tsunami inundation depth. Using the initial water displacement due to fault movement, we solved the 2D continuous equation and nonlinear long-wave equation nested as four grid data with mesh lengths of 270 m, 90 m, 30 m and 10 m. The results also show that the macrospatial correlation coefficients of the tsunami inundation depth have a tendency to decrease as the distance increases, whereas the rate of decrease in the macrospatial correlation coefficients on the land is greater compared to the results in the offshore region. This trend occurs because the run-up tsunamis on the land are affected in various ways by the bottom frictional resistance and attenuate faster compared to those in the offshore region. When we regressed the data using the least squares method, we observed that the macrospatial correlation coefficient  $\rho(x)$  of the tsunami inundation depth can be evaluated by the exponential function ( $\rho(x)=a\exp(bx)+c\exp(dx)$ ) with relatively high accuracy. The regression coefficients were  $a = 0.4555$ ,  $b = -0.1653$ ,  $c = 0.5434$ , and  $d = -0.007345$ , and the determination coefficient was 0.992. We also confirmed that the land gradient almost does not influence the results, although it is necessary to carry out further research on the possibility of fluctuations in the correlation coefficient due to changes in the assumed faults and seafloor topography in future studies. The results of this study can be used for a probabilistic tsunami risk assessment of real estate building portfolios by parties such as large companies, insurance companies, reinsurance companies, and real estate agencies.

*Keywords: Tsunami, Probabilistic tsunami risk assessment, Macrospatial correlation analysis*



## 1. Introduction

In a probabilistic disaster risk assessment for multiple buildings, we need to consider hazard correlation among site locations and damage correlation among multiple buildings because the probability distribution of aggregate damage for multiple buildings is affected. A risk assessment that does not consider the spatial correlation of hazards and damages may underestimate the risks posed by this correlation. Analyses that consider the spatial correlation of hazards have been relatively advanced in the fields of probabilistic seismic hazard assessment and probabilistic seismic risk assessment (PSHA and PSRA, respectively). In the case of PSRA, we generally assign various types of uncertainties to earthquake ground motions, ground characteristics, building response characteristics, and material strengths [1, 2, 3]. Regarding earthquake ground motion that is evaluated by an attenuation formula, we need to consider it as having a spatial correlation according to the relative distance [4, 5, 6, 7].

On the other hand, in the cases of probabilistic tsunami hazard assessment and probabilistic tsunami risk assessment (PTHA and PTRR, respectively), we also need to consider the spatial correlation characteristics of tsunami hazard and damage, but there have been no studies that evaluate this correlation. The aim of this study is to evaluate the spatial correlation coefficients of tsunami wave height and tsunami inundation depth according to the relative distance by using the results of tsunami numerical simulations with linear and nonlinear long-wave equations.

## 2. An evaluation method for the macrospatial correlation coefficient of tsunami hazards

Based on past studies [4, 5, 6, 7] that evaluated the spatial correlation coefficients of seismic ground motions, we evaluated the spatial correlation coefficients of tsunami phenomena. We define  $H_{sim}(r_i)$  as the maximum tsunami wave heights obtained by numerical simulations on a grid  $i$  and  $H_{pre}(r_i)$  as the predicted wave heights obtained by an evaluation formula on a grid  $i$ . Here,  $r_i$  is the shortest distance between each grid and the fault end point, or the coastline. The residual  $\varepsilon(r_i)$  between the numerical simulation result and the predicted value is evaluated as follows:

$$\varepsilon(r_i) = \log \left( \frac{H_{sim}(r_i)}{H_{pre}(r_i)} \right) \quad (1)$$

Using this residual  $\varepsilon(r_i)$ , we evaluate the variance in the residual ( $\sigma^2$ ) as follows:

$$\sigma^2 = \frac{1}{n} \sum_{i=1}^n (\varepsilon(r_i))^2 \quad (2)$$

Here,  $n$  is the number of target grids. Next, we evaluate the macrospatial correlation characteristics. The covariance of the  $i$ -th observation point 1 and observation point 2 can be written as follows from the definition of covariance:

$$\text{cov}(r_{i1}, r_{i2}) = \rho(r_{i1}, r_{i2}) \sigma(r_{i1}) \sigma(r_{i2}) \quad (3)$$

Here,  $\rho(r_{i1}, r_{i2})$  is a correlation coefficient between two points, and  $\sigma$  is a standard deviation in each grid. Assuming that the distance  $x$  between the two observation points 1 and 2 and the standard deviation  $\sigma$  are constant regardless of the point, we can reconstruct Eq. (3) to the Eq. (4):

$$\text{cov}(r_{i1}, r_{i2}) = \rho(x) (\sigma(r_i))^2 \quad (4)$$

$\text{cov}(r_{i1}, r_{i2})$  can also be written as follows by using the residual  $\varepsilon(r_i)$  between the numerical simulation result and the predicted value:



$$\text{cov}(r_{i1}, r_{i2}) = \frac{1}{N(x)} \sum_{i=1}^{N(x)} \varepsilon(r_{i1}) \varepsilon(r_{i2}) \quad (5)$$

Here,  $N(x)$  is the number of pairs in which the distance between the two points satisfies the following formula:

$$x - \frac{\Delta x}{2} \leq |r_{i1} - r_{i2}| \leq x + \frac{\Delta x}{2} \quad (6)$$

Here,  $\Delta x$  was set to 500 m for a numerical simulation of tsunami wave height and 10 m for a numerical simulation of tsunami inundation depth. We can derive the following formula from Eq. (4) and Eq. (5):

$$\rho(x) (\sigma(r_i))^2 = \frac{1}{N(x)} \sum_{i=1}^{N(x)} \varepsilon(r_{i1}) \varepsilon(r_{i2}) \quad (7)$$

Finally, the correlation coefficient  $\rho(x)$  with respect to the distance  $x$  between points 1 and 2 can be evaluated as follows:

$$\rho(x) = \frac{1}{(\sigma(r_i))^2 N(x)} \sum_{i=1}^{N(x)} \varepsilon(r_{i1}) \varepsilon(r_{i2}) \quad (8)$$

We can evaluate the spatial correlation coefficient  $\rho(x)$  of a tsunami wave height and tsunami inundation depth by calculating each variable on the right side of the formula. If we know the spatial correlation coefficient of the tsunami hazard, we can evaluate the spatial correlation coefficient of damage among multiple buildings using the relationship in the next paragraph and perform a stochastic damage evaluation for the building portfolio.

Here, we use two buildings as a risk assessment target. Let  $C_1$  and  $C_2$  be random variables for the strength of the two buildings, and let  $R_1$  and  $R_2$  be random variables for the hazard value (e.g., peak ground acceleration and tsunami inundation depth) at the two building sites. Assuming that  $C_1$  and  $C_2$  are independent but that  $R_1$  and  $R_2$  have a certain correlation, we obtain performance functions  $F_1$  and  $F_2$  as follows [2, 3]:

$$F_i = \frac{C_i}{R_i} \leftrightarrow \ln(F_i) = \ln(C_i) - \ln(R_i), \quad i = 1, 2 \quad (9)$$

The covariance of  $\ln(F_i)$  is now the same as the covariance of  $\ln(R_i)$ ; therefore, we obtain the following relation:

$$\text{cov}(\ln F_1, \ln F_2) = \text{cov}(\ln R_1, \ln R_2) \quad (10)$$

From this relation, the damage correlation coefficient  $\rho_{F_{12}}$  is as follows:

$$\rho_{F_{12}} = \frac{\text{cov}(\ln F_1, \ln F_2)}{\sqrt{\text{var}(\ln F_1)} \cdot \sqrt{\text{var}(\ln F_2)}} = \frac{\text{cov}(\ln R_1, \ln R_2)}{\sqrt{\text{var}(\ln R_1)} \cdot \sqrt{\text{var}(\ln R_2)}} \quad (11)$$

Here, we obtain the following equation:

$$\rho_{F_{12}} = \frac{\rho_{R_{12}} \zeta_{R_1} \zeta_{R_2}}{\sqrt{\zeta_{C_1}^2 + \zeta_{R_1}^2} \cdot \sqrt{\zeta_{C_2}^2 + \zeta_{R_2}^2}} \quad (12)$$



Here, let  $\rho_{R_{12}} (= \rho(x))$  be the hazard correlation coefficient with respect to the distance  $x$  between two points, let  $\zeta_n$  be the log normal standard deviation of  $n$  and let  $\zeta = \sqrt{\zeta_{Ci}^2 + \zeta_{Ri}^2}$  ( $i = 1, 2$ ) be the compound deviation. We obtain the following equation:

$$\rho_{F_{12}} = \frac{\rho_{R_{12}} \zeta_{R_1} \zeta_{R_2}}{\zeta^2} \quad (13)$$

For cases of earthquake hazard and damage assessment, we already know the values of  $\zeta^2$ ,  $\zeta_{R_1}$  and  $\zeta_{R_2}$  from past earthquake records and damage records; therefore, we can determine  $\rho_{F_{12}}$  when we evaluate  $\rho_{R_{12}}$ . However, in the case of tsunami hazards, there are no studies on the correlation coefficient of tsunami hazards. Based on the background, we evaluate the macrospatial correlation coefficient of a tsunami wave height and tsunami inundation depth in this study.

### 3. Numerical study on the macrospatial correlation of tsunami wave height

In this section, we evaluate the macrospatial correlation coefficient of a tsunami wave height according to the relative distance in an offshore region.

First, we establish a large virtual fault with a length of 250 km and a width of 100 km in the center of a virtual sea area with a water depth of 1000 m. The fault parameters of the large fault are a slip amount of 10 m, strike of 90°, dip of 15°, rake of 90° and fault depth of 1 km. The sea floor is horizontal, and terrain, such as islands, was not considered at all. Fig. 1 (a) shows the result of the initial water displacement of the tsunami due to fault movement by using Okada's equation [8]. The maximum water level was 4.56 m, and the minimum water level was -1.80 m. Using this initial water displacement as input data, we solved the continuous equation and linear long-wave equation (Eqs. (14), (15) and (16)) by using the staggered leapfrog method [9] and plane rectangular coordinates with a 500 m grid. We conducted the tsunami numerical simulation for 3 hours after the earthquake occurrence. Fig. 1 (b) shows the results of the maximum tsunami wave height for each grid. The maximum tsunami wave height in the region was 4.56 m, and the minimum tsunami wave height was 0.24 m.

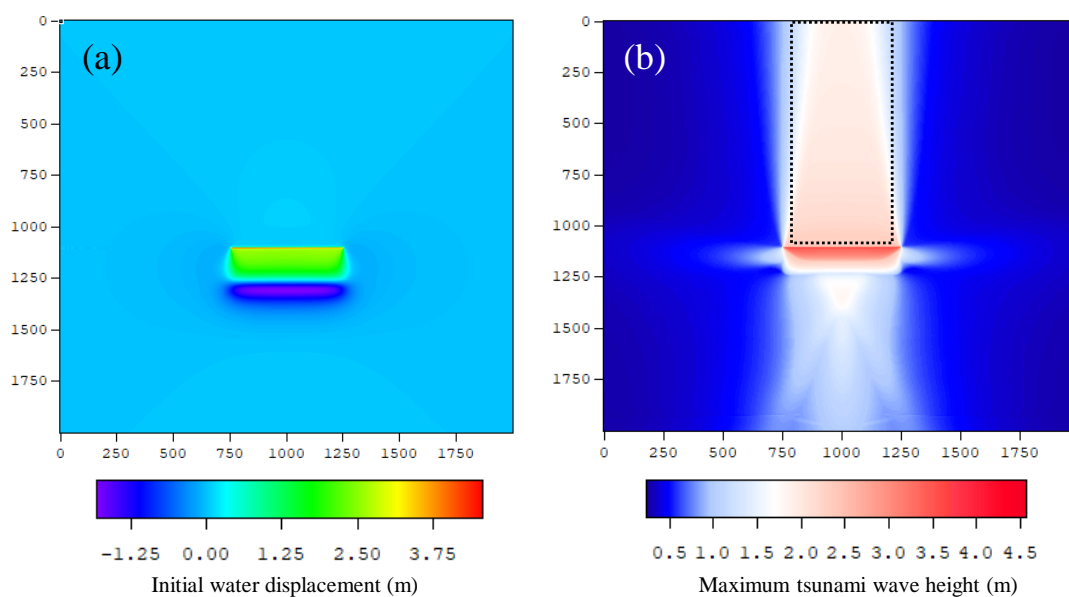


Fig. 1 (a) – Initial water displacement (m) due to fault movement, (b) – Maximum tsunami wave height (m)



The two-dimensional continuous equation and linear long-wave equation are as follows:

$$\frac{\partial \eta}{\partial t} + \frac{\partial M}{\partial x} + \frac{\partial N}{\partial y} = 0 \quad (14)$$

$$\frac{\partial M}{\partial t} + gD \frac{\partial \eta}{\partial x} = 0 \quad (15)$$

$$\frac{\partial N}{\partial t} + gD \frac{\partial \eta}{\partial y} = 0 \quad (16)$$

where  $\eta$  is the water level,  $D$  is the total water depth,  $g$  is the gravitational acceleration, and  $M$  and  $N$  are the flow fluxes in the  $x$  and  $y$  directions.

Fig. 1 (b) shows that the region with the high tsunami wave height appears in the 90° direction of the fault strike, clearly indicating the directivity of the tsunami accompanying the earthquake occurrence. In this study, we evaluate the correlation coefficient of the maximum tsunami wave height represented as the black dotted line in Fig. 1 (b) (horizontal axis: 800-1200, vertical axis: 1-1100) to take the directivity of the tsunami wave into consideration.

Fig. 2 (a) shows the attenuation characteristic of the tsunami wave height (distance from the earthquake fault vs. maximum tsunami wave height). We regressed the power function  $H = ax^b + c$  using the least squares method to determine the median values. The regression coefficients were  $a = -0.0508$ ,  $b = 0.4384$ , and  $c = 2.486$ , and the determination coefficient was 0.598. The standard deviation of the residual between the numerical simulation results and the predicted values from the power function was  $\sigma^2 = 0.022$  (see Fig. 3). Fig. 2 (b) shows the correlation coefficient results between two points using Eq. (8). The macrospatial correlation coefficients of the tsunami wave height tend to decrease as the distance between the two points increases, but the correlation coefficient is as high as approximately 0.74, even at a distance of approximately 100 km. This result occurs because there is almost no effect of sea bottom friction or topography that attenuates the tsunami wave height.

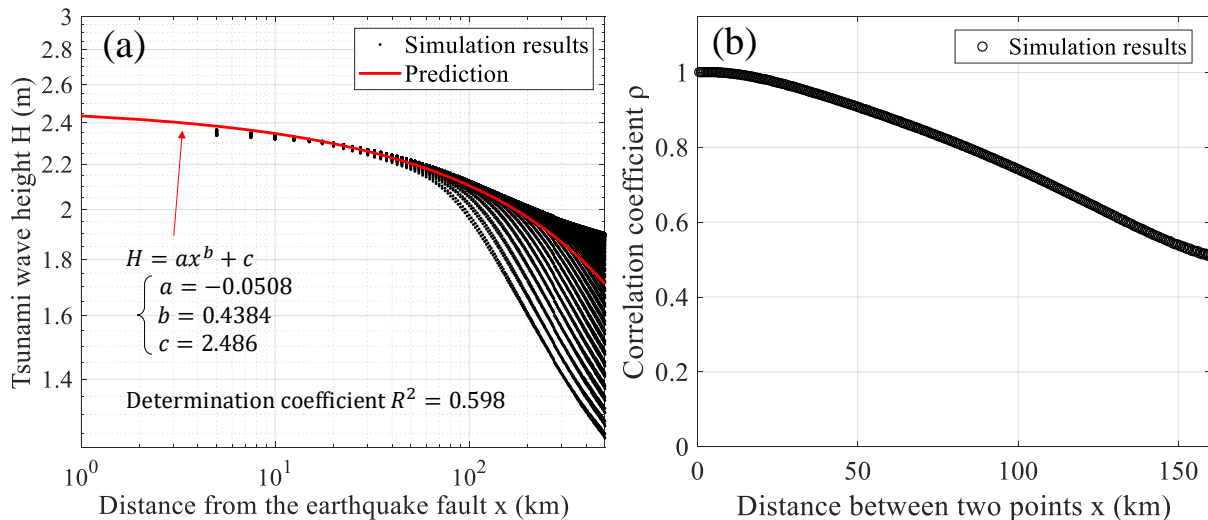


Fig. 2 (a) – Tsunami wave height attenuation, (b) – Correlation coefficient of the tsunami wave height

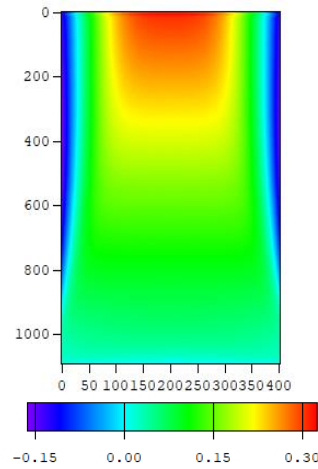


Fig. 3 The residual  $\varepsilon(r_i)$  between the numerical simulation results and the predicted values

#### 4. Numerical study of the macrospatial correlation of tsunami inundation depth

In this section, we evaluate the macrospatial correlation coefficient of the tsunami inundation depth according to the relative distance in the tsunami run-up region.

We first constructed the fault parameters of the earthquake of the Sagami trough, which has a large slip off the Kanto area in Japan, with reference to the earthquake parameter published by the Japan Seismic Hazard Information [10]. The moment magnitude (hereinafter referred to as  $M_w$ ) of the earthquake is 8.7, and there are 6,149 small faults. The slip distribution of the earthquake was set to three levels for the super large slip region (23.5 m), large slip region (11.7 m), and background slip region (1.94 m) (see Fig. 4 (a)) to satisfy the  $M_w$  8.7 of the earthquake based on the tsunami experiment method developed by the Headquarters for Earthquake Research Promotion [11]. Using the initial water displacement calculated from the earthquake parameters as input data, we solved the continuous equation and nonlinear long-wave equations (Eqs. (17), (18) and (19)) by using the staggered leapfrog method [9] and plane rectangular coordinates. We nested the four grid data with mesh lengths of 270 m, 90 m, 30 m and 10 m. We used the topography and roughness data published by the Cabinet Office and conducted the tsunami numerical simulation for 3 hours after the earthquake occurrence. Fig. 4 (b) shows the results of the tsunami inundation simulation in Zushi city, Kanagawa Prefecture. The maximum tsunami inundation depth was 8.71 m. The results of Fig. 4 (b) are almost consistent with the inundation area and depth of the tsunami hazard map published by Zushi city [12].

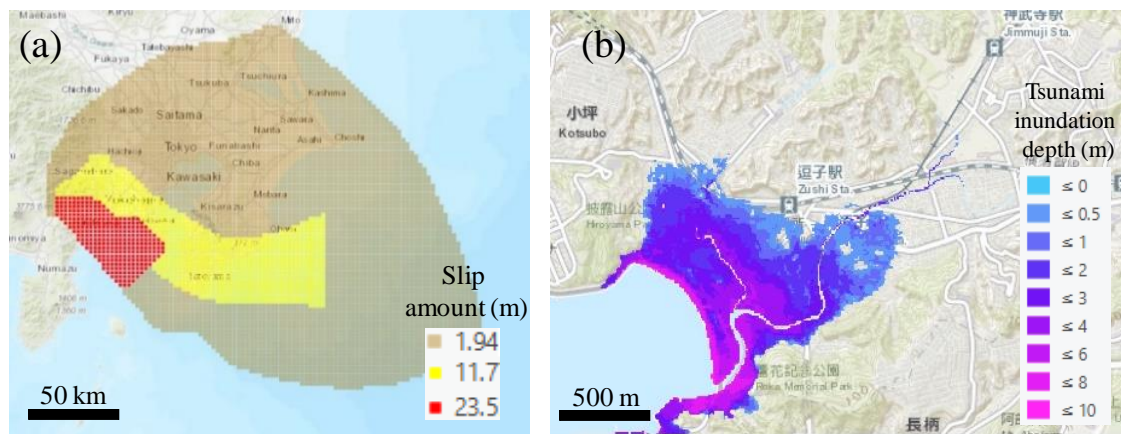


Fig. 4 (a) – A slip distribution of the Sagami trough earthquake around the Kanto region, (b) – Tsunami inundation depth distribution in Zushi city, Kanagawa Prefecture



The two-dimensional continuous equation and nonlinear long-wave equations are as follows:

$$\frac{\partial \eta}{\partial t} + \frac{\partial M}{\partial x} + \frac{\partial N}{\partial y} = 0 \quad (17)$$

$$\frac{\partial M}{\partial t} + \frac{\partial}{\partial x} \left[ \frac{M^2}{D} \right] + \frac{\partial}{\partial y} \left[ \frac{MN}{D} \right] + gD \frac{\partial \eta}{\partial x} + \frac{gn^2}{D^{7/3}} M \sqrt{M^2 + N^2} = 0 \quad (18)$$

$$\frac{\partial N}{\partial t} + \frac{\partial}{\partial x} \left[ \frac{MN}{D} \right] + \frac{\partial}{\partial y} \left[ \frac{N^2}{D} \right] + gD \frac{\partial \eta}{\partial y} + \frac{gn^2}{D^{7/3}} N \sqrt{M^2 + N^2} = 0 \quad (19)$$

where  $\eta$  is the water level,  $D$  is the total water depth,  $g$  is the gravitational acceleration,  $n$  is Manning's roughness coefficient and  $M$  and  $N$  are the flow fluxes in the  $x$  and  $y$  directions.

Fig. 5 (a) shows the relationship between the shortest distance from the coastline and the tsunami inundation depth. We regressed the exponential function  $H = a \exp(bx)$  using the least squares method to determine the median values. The regression coefficients were  $a = 4.911$  and  $b = -0.002078$ , and the determination coefficient was 0.538. The standard deviation of the residual  $\varepsilon(r_i)$  between the numerical simulation results and the predicted values from the exponential function is  $\sigma^2 = 0.794$ . Fig. 6 shows the spatial distribution of the residual  $\varepsilon(r_i)$  between the numerical simulation results and the predicted values. There is an area where the numerical calculation is overestimated along the river; in addition, there is an area where the estimation by the evaluation formula is overestimated at the tip of the run-up. Fig. 5 (b) shows the result of the correlation coefficients between two points. The macrospatial correlation coefficients of the tsunami inundation depth have a tendency to decrease as the distance between the two points increases, but the rate of decrease in the correlation coefficient in the tsunami run-up region is greater compared to the rate of decrease in the correlation coefficient of the tsunami wave height in the offshore region. The correlation coefficient decreased by approximately 0.78 at a distance of 1 mesh (10 m), indicating a low correlation of tsunami inundation depth. This result occurs because the run-up tsunamis were greatly affected by the bottom friction on the land and attenuated the inundation depth faster compared to the offshore area.

We regressed the following exponential function using the least squares method:

$$\rho(x) = a \exp(bx) + c \exp(dx) \quad (20)$$

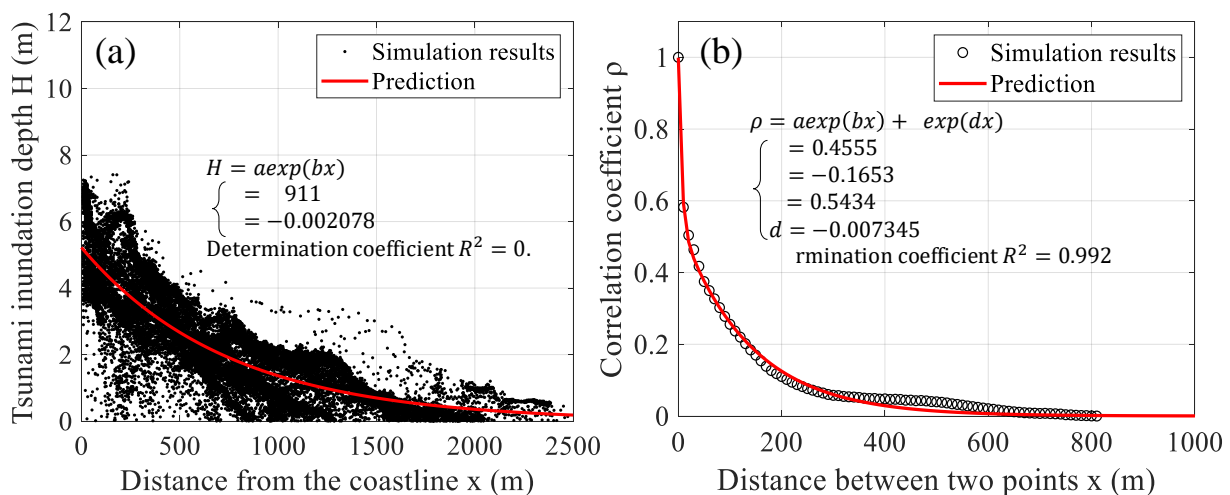


Fig. 5 (a) – Tsunami inundation depth attenuation, (b) – Correlation coefficient of the tsunami inundation depth

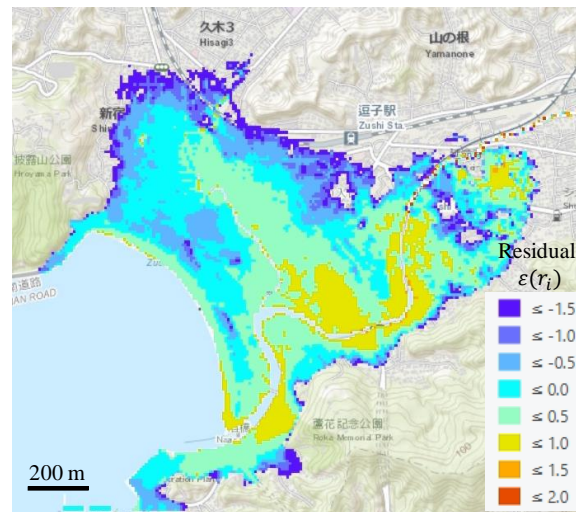


Fig. 6 – Spatial distribution of the residual  $\varepsilon(r_i)$  between the numerical simulation results and the predicted values

As a result, we obtained an evaluation formula with relatively high accuracy. The regression coefficients were  $a = 0.4555$ ,  $b = -0.1653$ ,  $c = 0.5434$ , and  $d = -0.007345$ , and the determination coefficient was 0.992. The correlation length was 53.2 m, and the correlation coefficient was equal to  $1/e$ .

However, the values of the spatial correlation coefficient could exhibit various fluctuations due to changes in the assumed faults, seabed and land topography. In the following simulation, we set the slope of the land to  $1/2$  or  $1/4$ , we re-evaluated the spatial correlation coefficient without changing the other conditions, and we determined how the values change.

Figs. 7 (a) and (b) show the simulation results of the tsunami inundation depth, and Figs. 8 (a) and (b) show the results of the relationship between the shortest distance from the coastline and the tsunami inundation depth. When the slope of the land is set to  $1/2$  or  $1/4$ , the tsunami penetrates and floods into the inland area where the terrain is more complicated. For this reason, the maximum tsunami wave height along the coastline is reduced by approximately 1-2 m. We regressed the exponential function  $H = a \exp(bx)$  using the least squares method to determine the median values. In the case with a  $1/2$  gradient, the regression coefficients were  $a = 5.221$  and  $b = -0.00134$ , and the determination coefficient was 0.716; in the case with a  $1/4$  gradient, the regression coefficients were  $a = 5.315$  and  $b = -0.00110$ , and the determination coefficient was 0.783. The standard deviation of the residual  $\varepsilon(r_i)$  between the numerical simulation results and the predicted values from the exponential function is  $\sigma^2 = 1.309$  in the case with a  $1/2$  gradient and is  $\sigma^2 = 0.825$  in the case with a  $1/4$  gradient. Fig. 9 (a) shows the result of the correlation coefficients between two points, and Fig. 9 (b) shows the difference in the correlation coefficient from the results of the control simulation without changing the gradient. From these figures, the fluctuation of  $\pm 0.05$  can be confirmed up to the distance of approximately 400 m between the two points; however, the spatial correlation coefficient hardly changes even if the topographic gradient is changed. This result indicates that we can evaluate the macrospatial correlation coefficient of tsunami inundation depth regardless of the land gradient by using Eq. (20). We performed a regression of Eq. (20) by using the least squares method for the two cases; in the case with a  $1/2$  gradient, the regression coefficients were  $a = 0.4931$ ,  $b = -0.006004$ ,  $c = 0.5053$ , and  $d = -0.1576$ , and the determination coefficient was 0.999; in the case with a  $1/4$  gradient, the regression coefficients were  $a = 0.4194$ ,  $b = -0.005941$ ,  $c = 0.5715$ , and  $d = -0.1022$ , and the determination coefficient was 0.992.

In the future, it is necessary to carry out further research on the possibility of fluctuations in the correlation coefficient due to changes in the assumed faults or seabed topography and to verify the validity of the evaluation formula.



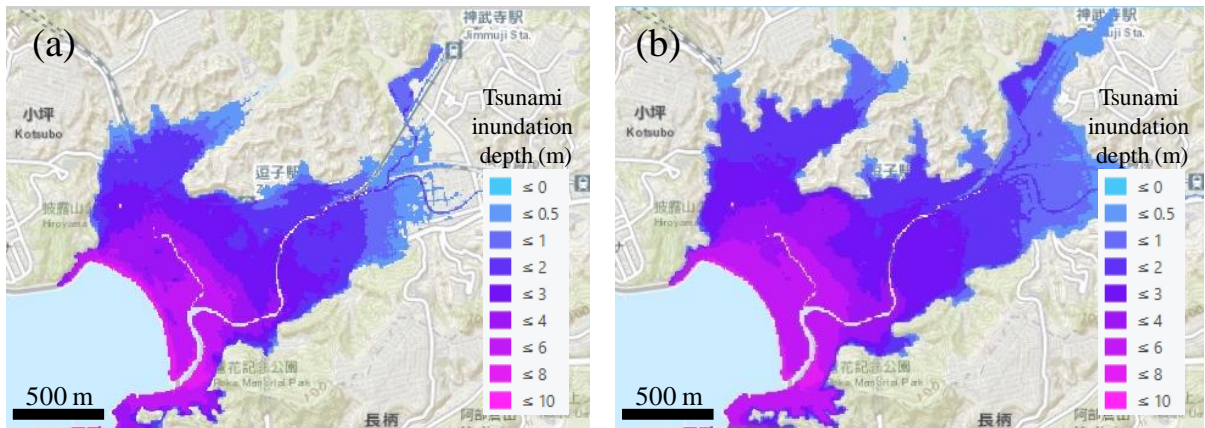


Fig. 7 (a) – Tsunami inundation depth in the case of a 1/2 gradient (b) – 1/4 gradient

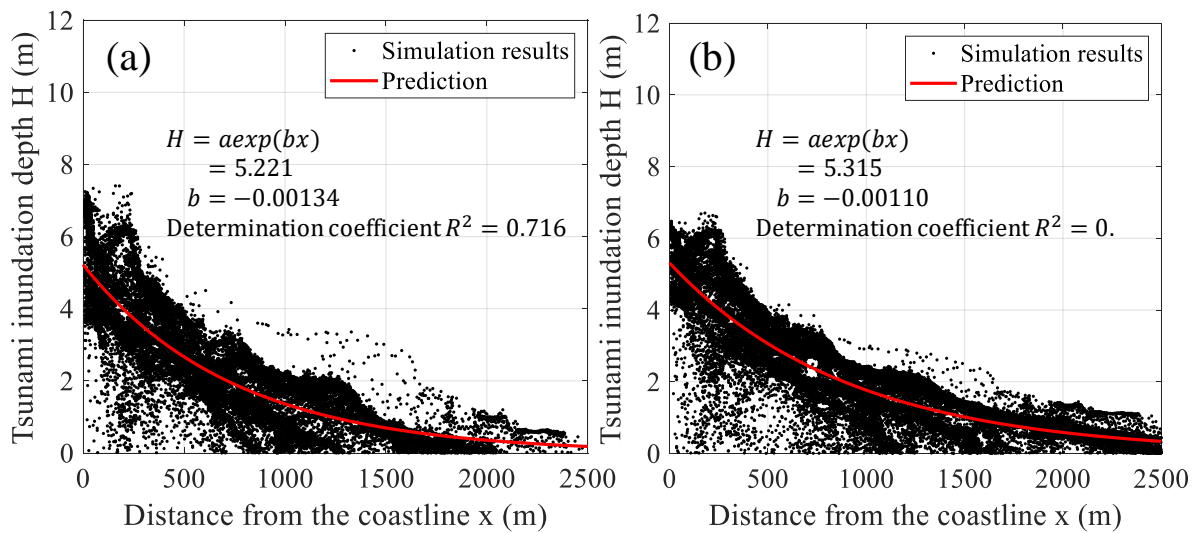


Fig. 8 (a) – Tsunami inundation depth attenuation in the case of changes with a 1/2 gradient, (b) – 1/4 gradient

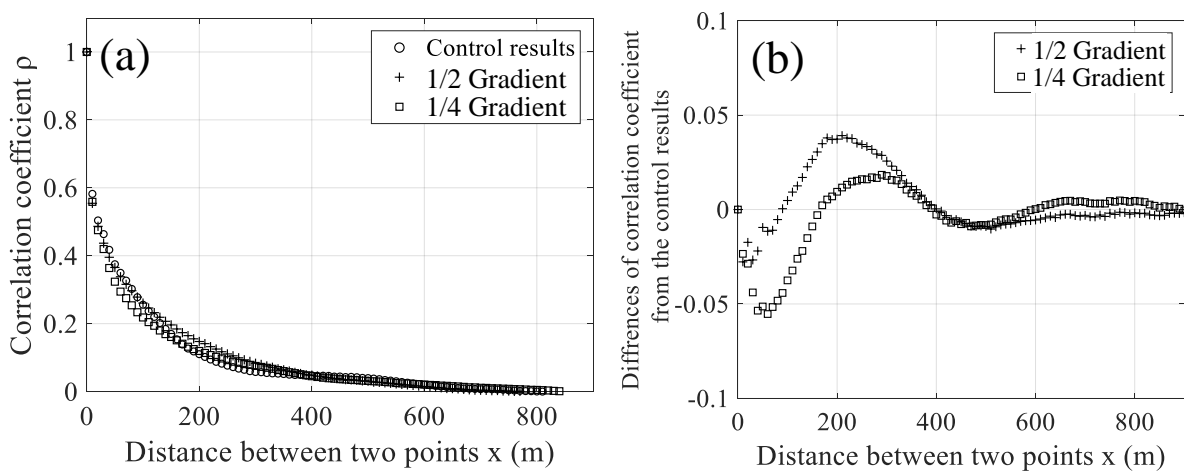


Fig. 9 (a) – Correlation coefficients of the tsunami inundation depth in the case of the control results, 1/2 gradient and 1/4 gradient, (b) – Differences in correlation coefficients from the control results



## 5. Conclusions

We determined the following spatial correlation features of tsunami wave height and tsunami inundation depth as the results of the tsunami numerical experiments using linear and nonlinear long-wave equations:

- The macrospatial correlation coefficients of the tsunami wave height in the offshore region have a tendency to decrease as the distance increases, but the correlation coefficient is as high as approximately 0.74 even at a distance of approximately 100 km.
- The macrospatial correlation coefficients of the tsunami inundation depth in the tsunami run-up region have a tendency to decrease as the distance increases, but the rate of decrease is greater compared to the macrospatial correlation coefficient results of the tsunami wave height in the offshore region. The correlation coefficient decreases by approximately 0.78 at a distance of 10 m, indicating a low correlation of the tsunami inundation depth. This result occurs because the run-up tsunamis on the land are affected in various ways by the bottom friction and attenuate faster compared to those in the offshore region.
- The macrospatial correlation coefficient of the tsunami inundation depth can be evaluated by the exponential function (Eq. (20):  $\rho(x) = aexp(bx) + cexp(dx)$ ) regardless of the land gradient.

The results of this study can be used for a probabilistic tsunami risk assessment of real estate building portfolios by parties such as large companies, insurance companies, reinsurance companies, and real estate agencies.

## 6. Acknowledgements

We thank the anonymous reviewers who provided us valuable comments and helped improve the manuscript. This research was partially supported by the funding from the Institute of Technology of Kanto Gakuin University.

## 7. References

- [1] Hayashi T, Fukushima S, Yashiro H (2006): EFFECTS OF THE SPATIAL CORRELATION BETWEEN GROUND MOTION INTENSITIES ON THE SEISMIC RISK OF PORTFOLIO OF BUILDINGS, *Journal of Structural and Construction Engineering*, **71** (600), 203-210.
- [2] Nakamura T (2008): A PORTFOLIO SEISMIC LOSS ESTIMATION CONSIDERING DAMAGE CORRELATION, *Journal of Structural and Construction Engineering*, **73** (623), 49-56.
- [3] Shizuma T, Nakamura T, Yoshikawa H (2009): EVALUATION FOR OUTAGE OF FACILITIES GROUP CONSIDERING SEISMIC DAMAGE CORRELATION, *Journal of Japan Society of Civil Engineers (A)*, **65** (2), 299-309.
- [4] Takada T, Shimomura T (2003): MACRO-SPATIAL CORRELATION OF SEISMIC GROUND MOTION ON STRONG MOTION RECORDS OF THE 1999 CHI-CHI EARTHQUAKE, *Journal of Structural and Construction Engineering*, **68** (565), 41-48.
- [5] Wang M, Takada T (2005): Macrospatial Correlation Model of Seismic Ground Motions. *Earthquake Spectra*, **21** (4), 1137-1156.
- [6] Itoi T (2011): Numerical Study on Macro-Spatial Correlation of Earthquake Ground Motion Intensity, *JCOSSAR 2011*.
- [7] Itoi T, Takada T (2012): Macro-spatial and inter-period correlation of spectral acceleration found in simulated ground motion, Proceedings of Fifth Asian-Pacific Symposium on Structural Reliability and its Applications (5APSSRA).



- [8] Okada Y (1985): SURFACE DEFORMATION DUE TO SHEAR AND TENSILE FAULTS IN A HALF-SPACE, *Bulletin of the Seismological Society of America*, **75** (4), 1135-1154.
- [9] Intergovernmental Oceanographic Commission (1997): Numerical Method of Tsunami Simulation with the Leap-Frog Scheme (Manuals and Guidelines 35), IUGG/IOC TIME PROJECT, UNESCO, <http://tsunami190245.tripod.com/tsh.pdf>, last access: 11 January 2020.
- [10] National Research Institute for Earth Science and Disaster Resilience (2018): Japan Seismic Hazard Information Station, <http://www.j-shis.bosai.go.jp/map/>, last access: 11 May 2018.
- [11] The Headquarters for Earthquake Research Promotion (2017): Tsunami prediction method for earthquakes with specified source faults (Tsunami Recipe), 33p.
- [12] Zushi city (2017): Tsunami hazard map in Zushi city, <https://www.city.zushi.kanagawa.jp/global-image/units/115865/1-20190606075726.pdf>, last access: 11 January 2020.